Orientations of side chains and adsorbed liquid crystal molecules on a rubbed polyimide surface studied by optical second harmonic generation

Seok-Cheol Hong, Masahito Oh-e, Xiaowei Zhuang,* and Y. R. Shen
Department of Physics, University of California, Berkeley, California 94720-7300

Jason J. Ge, F. W. Harris, and S. Z. D. Cheng
Department of Polymer Science, University of Akron, Akron, Ohio 44325-3909
(Received 7 September 2000; published 23 April 2001)

Surface second harmonic generation was used to obtain approximate orientational distributions of the side chains and the adsorbed liquid crystal (LC) molecules on a rubbed side-chain polyimide surface. Both the side chains and the LC molecules appear to be well aligned in the rubbing direction but tilted away from the surface in the antirubbing direction. The latter yields a negative pretilt angle in a homogeneously aligned LC film sandwiched between two such surfaces. The side chains and the LC molecules, however, have antiparallel orientations at the surface.

DOI: 10.1103/PhysRevE.63.051706 PACS number(s): 61.30.Gd, 68.35.Bs, 78.66.Qn, 61.41.+e

I. INTRODUCTION

Understanding liquid crystal (LC) alignment on mechanically rubbed surfaces is of great practical importance for the design of LC displays (LCD). The problem has been studied extensively in the past [1–8]. It is believed that rubbing aligns the surface polymer chains, which in turn align the LC layer adsorbed on the surface [1]. Recently, x-ray spectroscopy was used to measure quantitatively the alignment of surface polymer chains [6]. With sum-frequency vibrational spectroscopy and optical second harmonic generation, Wei *et al.* were able to obtain the orientational distributions of the surface polymer chains and the adsorbed LC monolayer and show that the two are well correlated [8]. However, details of LC alignment on different types of rubbed polymers are still not well understood.

One of the important design parameters for LCD is the pretilt angle of LC alignment in a film. To achieve a reasonable gray scale for LCD, a sufficiently large pretilt angle is needed. For example, for LCD in the supertwist-nematic operation mode, a pretilt as large as $\sim 15°$ is desired [9]. How to make an LC cell with a large pretilt has been a subject of immense interest to many researchers. Polymers with appropriate side chains appear to be a viable solution. While rubbing aligns the LC homogeneously, the side chains may help induce a large LC tilt angle. One such polymer is 6FDA-6CBO [this polymer is synthesized by a one-step polymerization method from 2,2′-bis(3,4-dicarboxyphenyl)hexafluoropropane dianhydride (6FDA) and 2,2′-bis(4′-cyanobiphenyl-4-oxyhexyloxy)-4,4′-diaminobiphenyl (6CBO)] [10]. Using optical second harmonic generation (SHG) and surface-enhanced Raman scattering (SERS), we found that rubbing indeed aligns the main chains along the rubbing direction, but it also causes the side chains to tilt away from the surface [10].

In this paper, we report our more detailed SHG measurements and analysis of the results from a rubbed 6FDA-6CBO surface and an LC monolayer (4′-*n*-pentyl-4 cyanobiphenyl, 5CB) adsorbed on it. SHG is a highly surface-specific technique [11]. With results from different input/output polarization combinations, it provides information on the surface molecular orientation. We have found that together with the main chains, the side chains are also aligned more or less along the rubbing direction but they are bent with the free terminals pointing towards the surface. The 5CB molecules adsorbed on the surface appear to align antiparallel to the side chains and therefore are oriented with a backward tilt with the CN terminal pointing out. This backward tilt of the surface LC molecular layer is responsible for the negative pretilt observed in the LC film sandwiched between substrates with a rubbed 6FDA-6CBO surface.

II. THEORETICAL BACKGROUND

The theory for surface SHG studies of LC has been described in detail elsewhere [2]. Here, for the convenience of later discussion, we present the essential parts. Surface SHG is generated in reflection from a surface nonlinear polarization $\vec{P}^{(2)}(2\omega)$ induced at an interface by the input field $\vec{E}(\omega)$, and the output intensity is given by

$$\begin{aligned} I(2\omega) &\propto |[\hat{e}_{2\omega}\cdot\overleftrightarrow{L}_{2\omega}]\cdot\vec{P}^{(2)}(2\omega)|^2 \\ &\propto |[\hat{e}_{2\omega}\cdot\overleftrightarrow{L}_{2\omega}]\overleftrightarrow{\chi}^{(2)}:[\overleftrightarrow{L}_{\omega}\cdot\hat{e}_{\omega}][\overleftrightarrow{L}_{\omega}\cdot\hat{e}_{\omega}]|^2|\vec{E}(\omega)|^4 \\ &\equiv |\chi^{(2)}_{\mathrm{eff}}(\Phi)|^2|\vec{E}(\omega)|^4, \end{aligned} \tag{1}$$

where $\hat{e}_{\Omega}$ is the unit polarization vector at frequency Ω, $\overleftrightarrow{L}_{\Omega}$ is the Fresnel factor, and Φ defines the azimuthal orientation of the sample in the laboratory coordinates. $\overleftrightarrow{\chi}^{(2)}$ is the surface nonlinear susceptibility tensor, and $\chi^{(2)}_{\mathrm{eff}}$, as defined, depends on Φ through $\hat{e}_{\Omega}$ with respect to the sample orienta-

*Present address: Department of Physics, Stanford University, Stanford, CA 94305-4060.

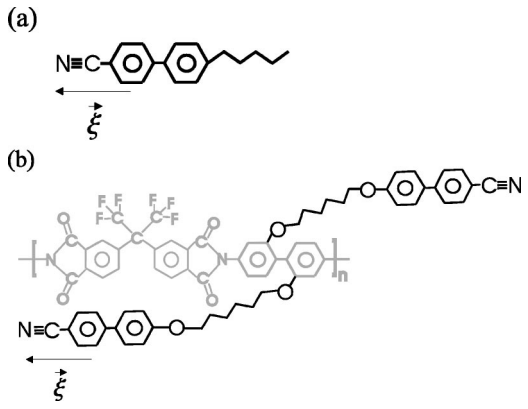

FIG. 1. Chemical structures of (a) 5CB and (b) 6FDA-6CBO.

tion. SHG measurements with different sample orientations allow us to determine $\chi^{(2)}_{\rm eff}(\Phi)$ for four different polarization combinations ($S_{\rm in}S_{\rm out}$, $S_{\rm in}P_{\rm out}$, $P_{\rm in}S_{\rm out}$, and $P_{\rm in}P_{\rm out}$). The relation between $\chi^{(2)}_{\rm eff}(\Phi)$ and $\vec{\vec{\chi}}^{(2)}$, which is given explicitly in Eq. (7) of Ref [2], then permits the deduction of all the nonvanishing $\chi^{(2)}_{ijk}$ elements.

As shown in Fig. 1, the side chains of 6FDA-6CBO are cyanobiphenyl molecules (6OCB), each of which connects to the main chain (6FDA) through an oxygen (O) atom. Like *n*CB, they have a strong nonlinearity and dominate the surface SHG from 6FDA-6CBO [10]. As rodlike molecules, their nonlinear polarizability tensor has a single dominant element $(\alpha^{(2)}_{\rm CBO})_{\xi\xi\xi}$ with $\hat{\xi}$ denoting a direction along the long molecular axis. For a surface of 6FDA-6CBO with $N_{\rm S}$ side chains per unit area oriented with an orientational distribution $f(\theta,\phi)$, the surface nonlinear susceptibility can be expressed as

$$(\chi^{(2)}_{\rm CBO})_{ijk}=N_{\rm S}(\alpha^{(2)}_{\rm CBO})_{\xi\xi\xi}\int(\hat{i}\cdot\hat{\xi})(\hat{j}\cdot\hat{\xi})(\hat{k}\cdot\hat{\xi})f(\theta,\phi)d\Omega, \tag{2}$$

where the angles θ and ϕ used to specify the orientation of $\hat{\xi}$ are defined in the inset of Fig. 2. For a rubbed surface with C_{1v} symmetry, there are six independent nonvanishing $\vec{\vec{\chi}}^{(2)}$ elements,

$$\chi^{(2)}_{xxx},\chi^{(2)}_{xyy}=\chi^{(2)}_{yxy}=\chi^{(2)}_{yyx},\quad \chi^{(2)}_{xzz}=\chi^{(2)}_{zxz}=\chi^{(2)}_{zzx},$$

$$\chi^{(2)}_{zxx}=\chi^{(2)}_{xzx}=\chi^{(2)}_{xxz},\quad \chi^{(2)}_{zyy}=\chi^{(2)}_{yzy}=\chi^{(2)}_{yyz},\chi^{(2)}_{zzz},$$

where $\hat{z}$ is along the surface normal and $\hat{x}$ and $\hat{y}$ are in the surface plane with $\hat{x}$ along the rubbing direction. Knowing the values of these $\chi^{(2)}_{ijk}$ and assuming

$$f(\theta,\phi)=A\exp\left[-\frac{(\theta-\theta_0)^2}{2\sigma^2}\right](1+d_1\cos\phi+d_2\cos 2\phi+d_3\cos 3\phi), \tag{3}$$

we can deduce from Eqs. (2) and (3) the five parameters θ_0, σ, d_1, d_2, and d_3. This then provides an approximate orientational distribution for the side chains.

For a 5CB monolayer on rubbed 6FDA-6CBO, SHG measurements yield the effective nonlinear susceptibility

$$|\chi^{(2)}_{\rm T,\,eff}(\Phi)|=|\chi^{(2)}_{\rm CBO,\,eff}(\Phi)+\chi^{(2)}_{\rm 5CB,\,eff}(\Phi)|$$
$$=\big||\chi^{(2)}_{\rm CBO,\,eff}(\Phi)|+|\chi^{(2)}_{\rm 5CB,\,eff}(\Phi)|e^{i\varphi}\big|. \tag{4}$$

Knowing $|\chi^{(2)}_{\rm CBO,\,eff}(\Phi)|$ from the measurement of the bare 6FDA-6CBO surface and measuring the relative phase φ, we can deduce $|\chi^{(2)}_{\rm 5CB,\,eff}(\Phi)|$ from Eq. (4). As discussed earlier, we can then find $(\chi^{(2)}_{\rm 5CB})_{ijk}$, from which, knowing that 5CB is also a rodlike molecule, we can use Eqs. (2) and (3) to find an approximate orientational distribution function for the 5CB monolayer.

III. EXPERIMENT

The samples of 6FDA-6CBO polymer films on fused quartz substrates were prepared by spin-coating. The polymer was first dissolved in cyclopentanone (10 wt. %) and filtered with a Teflon filter (0.45 μm). It was then spin-coated (2000 rpm, 30 sec) on the quartz plates, baked at 120 °C for 20 h, and rubbed once with a velvet cloth. The rubbing conditions were as follows: the rotational speed of a rubbing roller is 340 rpm, the translational speed of a substrate stage 1.7 mm/sec, and the pile impression 1 mm. Further rubbing decreased SHG from the sample. There was no further treatment of the samples after rubbing. The film thickness was about 640 nm. Its refractive indices measured by a commercial Sopra ellipsometer are 1.67 at 532 nm and $1.85+0.32i$ at 266 nm. The optical density (OD) of the film at 266 nm was 4.2. With our input laser beam at 532 nm from the air side, this makes SHG in reflection from the polymer-quartz interface negligible.

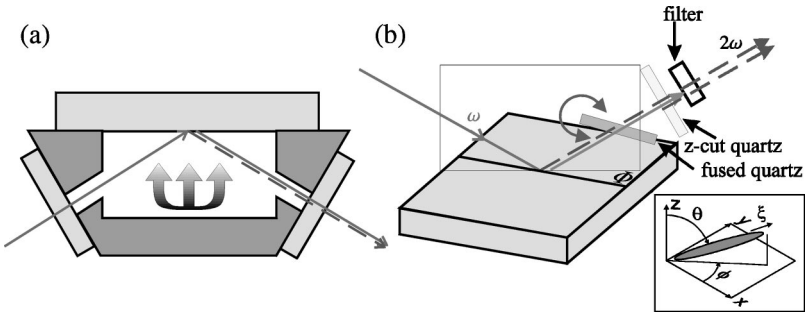

FIG. 2. Schematics showing the experimental arrangements for (a) 5CB deposition on a substrate and (b) SHG phase measurement. Fundamental and second harmonic beams are depicted by solid and dashed lines, respectively. Inset: Coordinate systems defining the orientation of a rodlike molecule.

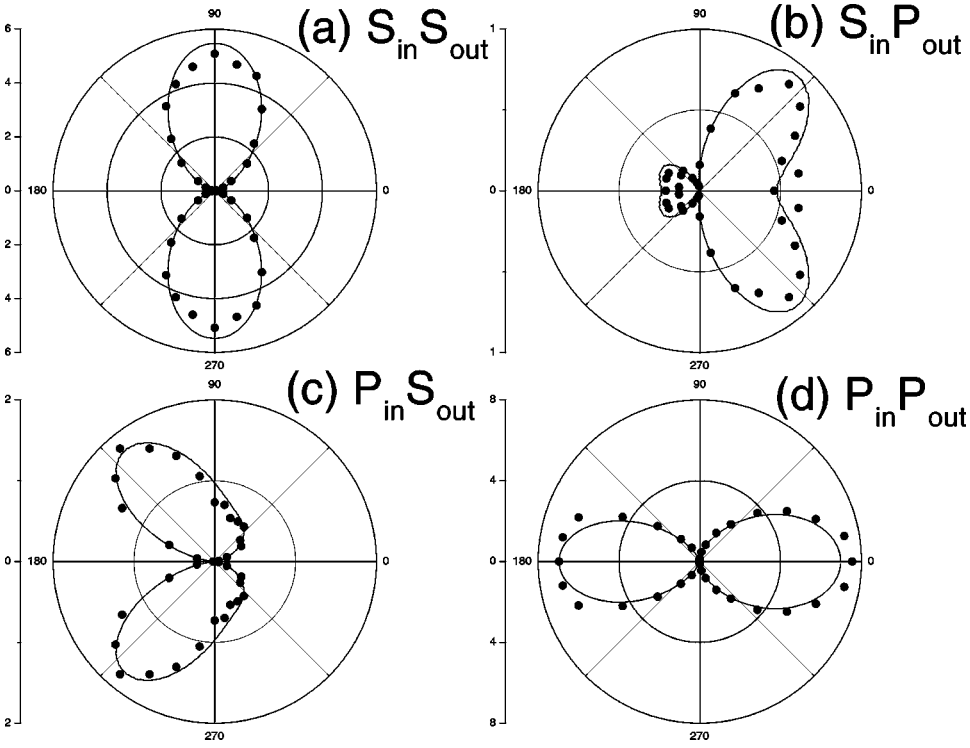

FIG. 3. Polar plots of $|\chi^{(2)}_{\mathrm{CBO,\,eff}}(\Phi)|^2$ (arbitrary units) versus Φ for (a) $S_{\mathrm{in}}S_{\mathrm{out}}$, (b) $S_{\mathrm{in}}P_{\mathrm{out}}$, (c) $P_{\mathrm{in}}S_{\mathrm{out}}$, and (d) $P_{\mathrm{in}}P_{\mathrm{out}}$ polarization combinations. Circles are experimental data and lines are fits.

The SHG experimental arrangement has been described elsewhere [2,4]. The sample was mounted on a 360° rotational stage and the dependence of SHG on the azimuthal angle Φ was measured for every 10° from 0° to 350°. The resultant $|\chi^{(2)}_{\mathrm{eff}}(\Phi)|$ then allowed us to deduce $\chi^{(2)}_{ijk}$ accurately. As the surface structure of 6FDA-6CBO could change with time after rubbing, we generally would wait for ~ 6 h before we started the SHG measurements. We also chose a few different laser spots on the surface to avoid possible laser damage. We collected SHG data for four different input/output polarization combinations: $S_{\mathrm{in}}S_{\mathrm{out}}$, $S_{\mathrm{in}}P_{\mathrm{out}}$, $P_{\mathrm{in}}S_{\mathrm{out}}$, and $P_{\mathrm{in}}P_{\mathrm{out}}$.

To study a 5CB monolayer on rubbed 6FDA-6CBO, the sample was prepared by thermal evaporation using an oven temperature of 60 °C [Fig. 2(a)]. *In situ* SHG was used to monitor the deposition of 5CB on the substrate. Formation of a monolayer is indicated by the leveling of the SHG signal [Fig. 7(b)], because beyond the monolayer, 5CB molecules on the surface form quadrupolar pairs and contribute little to SHG [12]. The sample was then mounted on a rotational stage, and SHG versus Φ was measured.

For SHG phase measurement, we introduced a fused quartz plate of $\frac{1}{8}$-in. thickness as a phase modulator and a thin (50-μm) *z*-cut crystalline quartz plate ($Q1$) as a reference SH generator in the reflected beam path, as shown in Fig. 2(b). A similar scheme was used previously [13]. The rotation of the fused quartz plate changes the optical path length and modulates the relative phase between the fundamental field and the reflected second harmonic field from the sample. The phase modulation causes the interference of SH fields from the sample and the reference quartz crystal ($Q1$) to vary and produces an interference pattern. By comparing the interference pattern with the one obtained by replacing the sample with another crystalline quartz reference ($Q2$), the phase of $\overleftrightarrow{\chi}^{(2)}$ of the sample with respect to that of the quartz reference ($Q2$) can be deduced.

IV. RESULTS AND ANALYSIS

Shown in Fig. 3 are the results of SHG measurements for the four polarization combinations on rubbed 6FDA-6CBO: $|\chi^{(2)}_{\mathrm{CBO,\,eff}}(\Phi)|^2$ versus Φ. As discussed in Sec. II, fitting the data (solid lines in Fig. 3) allows the determination of the six independent nonvanishing $(\chi^{(2)}_{\mathrm{CBO}})_{ijk}$ elements. We obtain

$$\chi^{(2)}_{xxx}:\chi^{(2)}_{xyy}:\chi^{(2)}_{xzz}:\chi^{(2)}_{zxx}:\chi^{(2)}_{zyy}:\chi^{(2)}_{zzz} = 1:0.23:0.036:-0.076:-0.020:-0.020$$

with errors of $\pm 5\%$, $\pm 20\%$, $\pm 10\%$, $\pm 25\%$, and $\pm 25\%$ for the five ratios, respectively. As we mentioned earlier, $(\chi^{(2)}_{\mathrm{CBO}})_{ijk}$ originates mainly from the 6CBO side chains. However, it was found in a similar polyimide (6FDA-PFMB, which has the same backbone but no side chains [10]) that the field discontinuity at the surface (along $\hat{z}$) contributes a value of 0.012 to $\chi^{(2)}_{zzz}$. This is significant compared to the above value of -0.020 for $(\chi^{(2)}_{\mathrm{CBO}})_{zzz}$ and must be subtracted from the latter if we are only interested in the contribution of the side chains to $(\chi^{(2)}_{\mathrm{CBO}})_{zzz}$ for the deduction of the distribution function $f(\theta,\phi)$ for the side chains. Contributions of the field discontinuity to the other $(\chi^{(2)}_{\mathrm{CBO}})_{ijk}$ elements are much weaker and can be neglected. We can then use the values of $(\chi^{(2)}_{\mathrm{CBO}})_{ijk}$ to determine $f(\theta,\phi)$ following Eqs. (2) and (3). The deduced parameters for $f(\theta,\phi)$ are listed in Table I. It is interesting to note that the parameter d_1 is negative. This implies that the 6CBO side chains are aligned

TABLE I. Parameters in orientational distribution function $f(\theta,\phi)$ for 6FDA-6CBO and 5CB monolayer.

	6FDA-6CBO	5CB
θ_0	86.5 ± 1.0	81.4 ± 1
σ	9.5 ± 1.0	10.5 ± 0.5
d_1	-1.4 ± 0.4	-0.81 ± 0.1
d_2	1.2 ± 0.2	0.79 ± 0.05
d_3	-0.38 ± 0.15	-0.20 ± 0.05

opposite to the rubbing direction. From $\int f(\theta,\phi)\ \sin\theta\, d\theta$, we can obtain the azimuthal distribution of the side chains, as depicted in Fig. 4.

The SHG intensity measurements cannot distinguish between the two possible molecular orientations of the side chains in Figs. 5(a) and 5(b). To resolve the ambiguity, we need a phase measurement. We consider here the phase of $\chi^{(2)}_{xxx}$. The side chains with opposite orientations illustrated in Figs. 5(a) and 5(b) should have a 180° phase difference in $\chi^{(2)}_{xxx}$ [as can be seen explicitly in Eq. (2) with $\hat{\xi}$ replaced by $-\hat{\xi}$]. We can compare the measured phase of $\chi^{(2)}_{xxx}$ for the 6CBO side chains with that for a 5CB monolayer adsorbed on a polyimide without side chains ($P6$) [3,4]. The latter is known to have 5CB molecules oriented with the CN terminal facing the surface [Fig. 5(c)]. As is seen from the measured interference patterns for the two cases in Figs. 5(d) and 5(e), the phase of $\chi^{(2)}_{xxx}$ of 5CB on $P6$ is opposite to that of 6CBO. The correct orientation of the 6CBO side chains therefore must be the one shown in Fig. 5(a). We also found that the phases of $\chi^{(2)}_{zxx}$ for the 6CBO side chains and the 5CB monolayer are the same, consistent with the pictures in Figs. 5(a) and 5(c). As we shall see later, this orientation of the 6CBO side chains is responsible for the observed negative pretilt of the LC bulk alignment.

The results of $|\chi^{(2)}_{T,\mathrm{eff}}(\Phi)|^2$ versus Φ from SHG measurements on a 5CB monolayer on rubbed 6FDA-6CBO with four polarization combinations are given in Fig. 6. In order

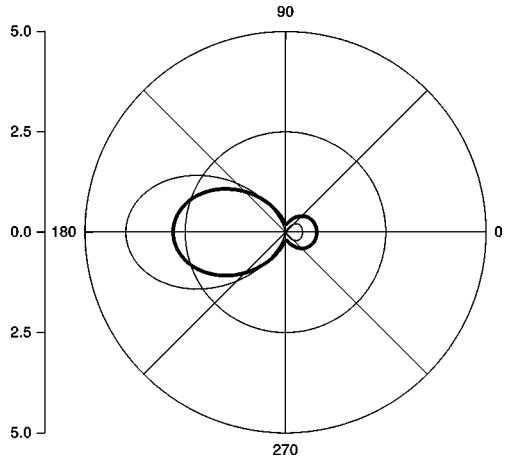

FIG. 4. Azimuthal orientational distributions of side chains (thin line) and 5CB molecules in an adsorbed monolayer (thick line) on a rubbed 6FDA-6CBO surface.

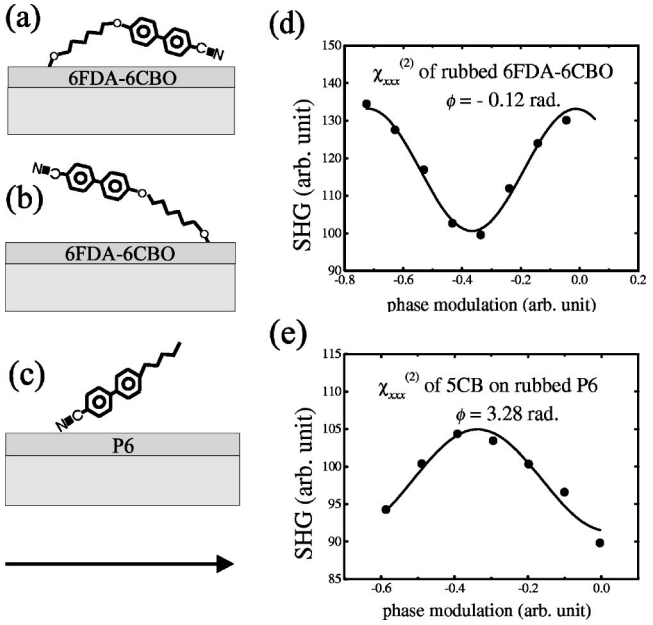

FIG. 5. Schematics describing the two possible orientations of the 6CBO side chains in (a) and (b) and the orientation of 5CB molecules adsorbed on a polyimide (P6) surface in (c). The experimental data and the line fits in (d) and (e) describe the results of SHG phase measurements of $(\chi^{(2)}_{\mathrm{CBO}})_{xxx}$ and $(\chi^{(2)}_{\mathrm{5CB}})_{xxx}$, respectively. The arrow denotes the rubbing direction.

to determine $\chi^{(2)}_{\mathrm{5CB,\,eff}}(\Phi)$, we used Eq. (4), in which $|\chi^{(2)}_{\mathrm{CBO,\,eff}}(\Phi)|$ was already obtained and φ measured with SHG phase measurement is 0.26 ± 0.3 rad. Within the error of our measurement, φ was found to be indepedent of input/output polarization combinations or sample orientations, as expected from the rodlike molecules. Thus, fitting of the measured $|\chi^{(2)}_{T,\mathrm{eff}}(\Phi)|^2$ with $(\chi^{(2)}_{\mathrm{5CB}})_{ijk}$ as adjustable parameters allows us to determine the six nonvanishing $(\chi^{(2)}_{\mathrm{5CB}})_{ijk}$. After normalization against $(\chi^{(2)}_{\mathrm{CBO}})_{xxx}$, they are

$$\chi^{(2)}_{xxx}:\chi^{(2)}_{xyy}:\chi^{(2)}_{xzz}:\chi^{(2)}_{zxx}:\chi^{(2)}_{zyy}:\chi^{(2)}_{zzz}$$
$$=-0.81:-0.191:-0.028:0.23:0.101:0.041$$

with errors of $\pm4\%$, $\pm10\%$, $\pm20\%$, $\pm5\%$, $\pm10\%$, and $\pm12\%$, respectively. From these values of $(\chi^{(2)}_{\mathrm{5CB}})_{ijk}$, we can again use Eqs. (2) and (3) to find $f(\theta,\phi)$ for the 5CB monolayer. The deduced parameters for $f(\theta,\phi)$ of 5CB are also listed in Table I. We note that $(\chi^{(2)}_{\mathrm{5CB}})_{xxx}$ and $(\chi^{(2)}_{\mathrm{CBO}})_{xxx}$ have opposite signs, indicating that the 5CB molecules and the CBO side chains have antiparallel orientations along the rubbing direction [Fig. 7(a)]. This is well confirmed by the *in situ* SHG measurement monitoring the 5CB deposition on 6FDA-6CBO described in Fig. 7(b). The decay of $|(\chi^{(2)}_{T,\,\mathrm{eff}})_{xxx}|^2$ with 5CB deposition is a clear indication that the adsorbed 5CB molecules and the 6CBO side chains have opposite orientations. As shown in Fig. 4, the azimuthal distribution of the 5CB monolayer obtained from $\int f(\theta,\phi)\sin\theta d\theta$ is well correlated with that of the side chains.

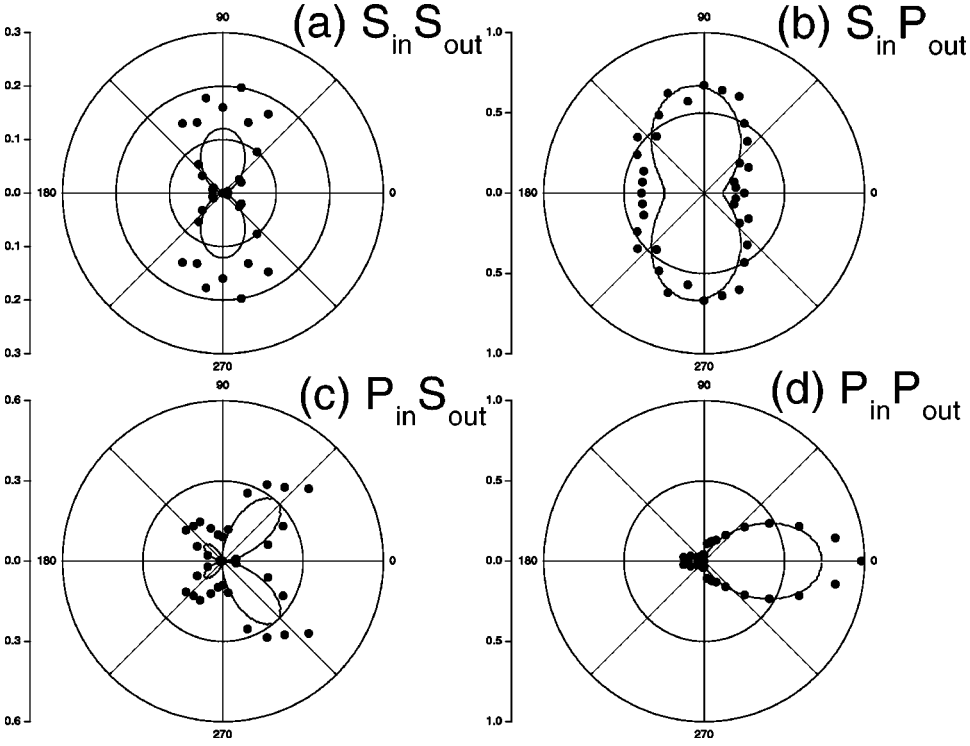

FIG. 6. Polar plots of $|\chi^{(2)}_{T,\mathrm{eff}}(\Phi)|^2$ (arbitrary units) versus Φ for (a) $S_{\mathrm{in}}S_{\mathrm{out}}$, (b) $S_{\mathrm{in}}P_{\mathrm{out}}$, (c) $P_{\mathrm{in}}S_{\mathrm{out}}$, and (d) $P_{\mathrm{in}}P_{\mathrm{out}}$ polarization combinations. Circles are experimental data and lines are fits.

A 5CB LC film sandwiched between two substrates coated with rubbed 6FDA-6CBO (Fig. 8) appeared to be well aligned homogeneously along the rubbing direction. From an ellipsometry measurement (Ref. [14]), the bulk pretilt angle was found to be $\alpha_b = -8.7°$. This negative pretilt angle is induced through LC molecular correlation by the orientation of molecules in the surface LC monolayers, which is antiparallel to the rubbing direction (Fig. 8). Assuming boundary surfaces fully covered with 5CB molecules with the orientational distribution specified in Table I, we can use the Landau–de Gennes theory to calculate the pretilt angle [4]. We found $\alpha_b = -4.4°$. The discrepancy between theory and experiment is presumably because, in reality, the boundary surfaces are composed of a mixture of oriented 5CB molecules and 6CBO side chains.

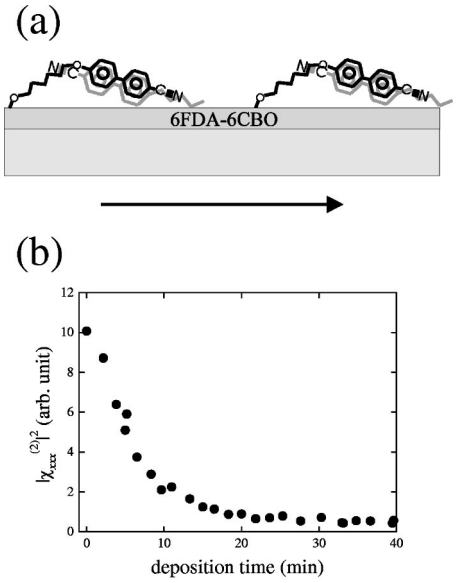

FIG. 7. (a) Schematic showing the orientations of adsorbed 5CB molecules and 6CBO side chains on a rubbed 6FDA-6CBO surface. The arrow denotes the rubbing direction. (b) $|(\chi^{(2)}_{T,\mathrm{eff}})_{xxx}|^2$ as a function of 5CB evaporation time obtained by *in situ* SHG monitoring of 5CB deposition on 6FDA-6CBO.

V. DISCUSSION

SHG is highly surface-specific and sensitive, but is not necessarily helpful in the determination of surface molecular orientation unless the molecule is highly symmetric [2]. Fortunately, this is the case for both 6CBO side chains and 5CB molecules. The second-order nonlinear polarizabilities for both 6CBO and 5CB are dominated by the cyanobiphenyl chromophores, which appear to have no strongly preferred orientation about their long molecular axes. Thus they can be treated as rodlike molecules and, as shown in the preceding section, SHG can be used to determine approximate orientational distributions of the chromophores.

It is known that rubbing can align the main chains of a polymer at the surface [6,8,15,16]. This has been found to be

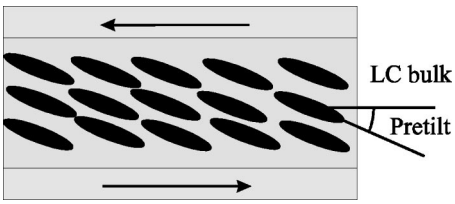

FIG. 8. Schematic describing the negative pretilt angle of a 5CB film sandwiched between two rubbed 6FDA-6CBO surfaces. The arrows denote the rubbing directions on the two substrates.

true for a number of polyimides including 6FDA-6CBO. What we have observed here in addition is that the side chains are also aligned by rubbing, which is not always the case [17]. The reason is that the polar 6CBO side chains here are connected to the main chains through a $(CH_2)_6$ section that can be bent by creation of *trans-cis* defects. The chromophores are expected to orient along the rubbing direction. Since the terminal CN of 6CBO has an attractive interaction with the polyimide main chain, the chromophores would have a polar orientation with a tilt in the direction antiparallel to rubbing [Fig. 5(a)], as we have observed.

On polyimides without side chains, 5CB molecules are known to adsorb with the CN terminal anchored on the main chain. With the 6CBO side chains, however, this is no longer the case. We now have the polar orientation of adsorbed 5CB molecules inverted, i.e., the CN terminal is pointing away from the surface. Apparently, the interaction between 5CB and 6CBO chromophores must have dominated and favored the antiparallel pair interaction geometry normally observed in an LC bulk. Rubbing aligns the 6CBO side chains, which in turn aligns the adsorbed 5CB molecules. The azimuthal orientational distributions of 6CBO and 5CB chromophores are therefore correlated (Fig. 4).

The pretilt angle of a homogeneously aligned LC film is determined by the molecular orientations in the boundary layers. In our case, the observed negative pretilt is obviously induced by the orientations of 6CBO and 5CB at the surface, which are opposite to the rubbing direction. As to a quantitative estimate of the pretilt, unfortunately we do not yet know how to describe properly the orientational boundary condition for LC presented by a mixed monolayer of 6CBO and 5CB.

The goal of many workers on LCD is to have a large, controllable pretilt angle. Our work here indicates that this may be possible with side-chain polyimides if the side chains have an appropriate structure. For a large pretilt, we need side chains that can be aligned by rubbing and have a large tilt away from the surface. They must also interact with LC molecules sufficiently strongly so that they can effectively align the latter. We can image, for example, a modification of 6FDA-6CBO. Instead of attaching 6CBO directly to the 6FDA main chain, let it be attached through a stiff molecular stem projecting vertically out from the main chain and from the surface. This way, 6CBO side chains retain all their characteristic features for LC alignment, but the additional spacing between 6CBO and the main chain, effected by the molecular stem, would allow 6CBO to have a larger tilt at the surface. Varying the length of the stem could change the tilt angle of 6CBO and hence the pretilt of the LC film.

VI. CONCLUSION

Surface SHG allowed the determination of approximate orientational distributions of 6CBO side chains on a rubbed 6FDA-6CBO surface and 5CB molecules adsorbed on the surface. There is a strong correlation between the two. Both are highly anisotropic, preferentially aligned along the rubbing direction. The molecular tilts away from the surface, however, are in the antirubbing direction. This leads to the negative pretilt we observed in the homogeneously aligned LC film sandwiched between substrates coated with rubbed 6FDA-6CBO. The orientations of 6CBO and 5CB at the surface were found to be antiparallel, as one would expect from the pair interaction geometry of such molecules. Our results here provide us with some insight on possible exploitation of side-chain polymers to control the pretilt angle of an LC display cell.

ACKNOWLEDGMENTS

We would like to acknowledge useful discussions with Xing Wei for the SHG phase measurement. This work was supported by the National Science Foundation through Grant No. DMR-9704384 and the Technology Center of Advanced Liquid Crystalline Optical Materials (ALCOM, DMR-9157738). M.O. gratefully acknowledges Hitachi, Ltd. for financial support.

[1] J. M. Geary, J. W. Goodby, A. R. Kmetz, and J. S. Patel, J. Appl. Phys. **62**, 4100 (1987).

[2] M. B. Feller, W. Chen, and Y. R. Shen, Phys. Rev. A **43**, 6778 (1991); W. Chen, M. B. Feller, and Y. R. Shen, Phys. Rev. Lett. **63**, 2665 (1989).

[3] D. Johannsmann, H. Zhou, P. Sonderkaer, H. Wierenga, B. O. Myrvold, and Y. R. Shen, Phys. Rev. E **48**, 1889 (1993).

[4] X. Zhuang, L. Marrucci, and Y. R. Shen, Phys. Rev. Lett. **73**, 1513 (1994); M. Barmentlo, R. W. J. Hollering, and N. A. J. M. van Aerle, Phys. Rev. A **46**, R4490 (1992).

[5] K. Shirota, M. Yaginuma, T. Sakai, K. Ishikawa, H. Takezoe, and A. Fukuda, Appl. Phys. Lett. **69**, 164 (1996); T. Sakai, J. Yoo, Y. Kinoshita, K. Ishikawa, H. Takezoe, A. Fukuda, T. Nihira, and H. Endo, *ibid.* **71**, 2274 (1997).

[6] M. G. Samant, J. Stöhr, H. R. Brown, T. P. Russell, J. M. Sands, and S. K. Kumar, Macromolecules **29**, 8334 (1996); K. Weiss, C. Wöll, E. Böhm, B. Fiebranz, G. Forstmann, B. Peng, V. Scheumann, and D. Johannsmann, *ibid.* **31**, 1930 (1998); J. Stöhr, M. G. Samant, A. Cossy-Favre, J. Diaz, Y. Momoi, S. Odahara, and T. Nagata, *ibid.* **31**, 1942 (1998); A. Cossy-Favre, J. Diaz, Y. Liu, H. R. Brown, M. G. Samant, J. Stöhr, A. J. Hanna, S. Anders, and T. P. Russell, *ibid.* **31**, 4957 (1998).

[7] K.-W. Lee, A. Lien, J. H. Stathis, and S.-H. Paek, Jpn. J. Appl. Phys., Part 1 **36**, 3591 (1997); S.-H. Paek, C. J. Durning, K.-W. Lee, and A. Lien, J. Appl. Phys. **83**, 1270 (1998).

[8] X. Wei, X. Zhuang, S.-C. Hong, T. Goto, and Y. R. Shen, Phys. Rev. Lett. **82**, 4256 (1999); X. Wei, S.-C. Hong, X. Zhuang, T. Goto, and Y. R. Shen, Phys. Rev. E **62**, 5160 (2000).

[9] V. G. Chigrinov, V. V. Belyaev, S. V. Belyaev, and M. F. Grebenkin, Zh. Éksp. Teor. Fiz. **77**, 2081 (1979) [Sov. Phys. JETP **50**, 994 (1979)].

[10] J. J. Ge, G. Xue, F. Li, K. W. McCreight, S. Wang, F. W.

Harris, S. Z. D. Chang, X. Zhuang, S.-C. Hong, and Y. R. Shen, Macromol. Rapid Commun. **19**, 619 (1998).
[11] Y. R. Shen, Annu. Rev. Phys. Chem. **40**, 327 (1989).
[12] C. S. Mullin, P. Guyot-Sionnest, and Y. R. Shen, Phys. Rev. A **39**, 3745 (1989).
[13] J. Y. Huang and A. Lewis, Biophys. J. **55**, 835 (1989).
[14] G. Baur, V. Wittwer, and D. W. Berreman, Phys. Lett. **56A**, 142 (1976); K. Han, T. Miyashita, and T. Uchida, Jpn. J. Appl. Phys., Part 2 **32**, L277 (1993).
[15] D. Kim, M. Oh-e, and Y. R. Shen (unpublished).
[16] M. Oh-e, S.-C. Hong, and Y. R. Shen, J. Phys. Chem. B **104**, 7455 (2000).
[17] M. Oh-e, A. I. Lvovsky, X. Wei, and Y. R. Shen, J. Chem. Phys. **113**, 8827 (2000).